THE ENERGY STATES IN $Ga_{1-x}Al_xAs/GaAs$ QUANTUM WELL WIRE LATTICE UNDER THE EFFECT OF EXTERNAL ELECTRIC FIELD

Bahadır BEKAR[*1]

*1*Keşan Vocational School, Trakya University, Keşan, Edirne, TÜRKİYE*

Abstract

In the lattice consisting of three quantum wires, the effect of the external electric field applied on the energy states of the electron is the focus of this study. The energy states and wave functions of the electron were calculated using the finite difference method with the effective mass approach. It was found that the energy states exhibit different behavior when the diameters of the quantum wires are considered as the same and different. When an electric field was applied to both quantum wire lattices, the electron's energy states showed interesting changes.

Keywords: Quantum Wire, Electric Field, Energy Crossing

HARİCİ ELEKTRİK ALANI ETKİSİ ALTINDA $Ga_{1-x}Al_xAs/GaAs$ KUANTUM KUYU TEL ÖRGÜSÜNDEKİ ENERJİ DURUMLARI

Öz

Üç kuantum telinden oluşan örgüde, uygulanan dış elektrik alanın elektronun enerji durumları üzerindeki etkisi bu çalışmanın odak noktasıdır. Etkin kütle yaklaşımı ile sonlu farklar yöntemi kullanılarak elektronun enerji durumları ve dalga fonksiyonları hesaplanmıştır. Kuantum tellerinin çaplarının aynı ve farklı olduğu düşünüldüğünde enerji durumlarının farklı davranışlar sergiledikleri bulunmuştur. Her iki kuantum tel kafesine bir elektrik alanı uygulandığında, elektronun enerji durumları ilginç değişiklikler gösterdi.

Anahtar Kelimeler: Kuantum Teli, Elektrik Alanı, Enerji Geçişi

Sorumlu Yazar: Bahadır BEKAR, bahadirbekar@trakya.edu.tr

1. INTRODUCTION

After the discovery of semiconductor, properties of low-dimensional semiconductor structures have been attracted attention. Many electronic devices have been designed by combining different semiconductor materials. These devices have become manufactured at nano-structure scales with the developments in production technology. Thus, a transition was made to quantum wells, quantum wires and quantum dots. As a result, it has caused many macro-sized electronic elements to be produced in nano-sizes. The electronic properties of these structures under electric field have also investigated [1-4]. Magnetic field [5-6], hydrostatic pressure [7-9], temperature [10,11], and laser [12-15], its behavior under external influences has also been added to intensive work on low-dimensional structures.

Another research area was the investigations made by adding foreign atoms to original semiconductors [3,5,6]. In addition, it was observed that the results differ for each structure when these external fields are effected on geometrically different quantum structures [16-19]. The effect of dielectric constants of materials on quantum structures was investigated [20].

In this study, we have investigated the energy levels of the electron by applying an electric field to the states of the same and different diameters of the GaAs material in the triple quantum wire. The calculation method of the structure under the electric field is given in section 2.; in the section 3, the results of the calculated energy states and probabilities of finding wave functions are given.

2. MATERIALS AND METHOD

Figure 1 shows the xy-plane cross section of the $Ga_{1-x}Al_xAs/GaAs$ quantum wire lattice. In the effective mass approximation, the time-independent Schrödinger equation for an electron in Quantum well wires (QWW), in the presence of the electric field is given by:

$$H = -\frac{\hbar^2}{2m^*}\left(\frac{\partial^2}{\partial x^2} + \frac{\partial^2}{\partial y^2}\right) + |e|Fx + V_0(x,y) \tag{1}$$

Where, e is the electron charge, m^* is electron effective mass and F is the electric field strength in units of kV/cm applied in the +x-axis direction. Eq.1, Rydberg energy unit $R^* = \frac{m^* e^4}{2\hbar^2 \varepsilon^2}$ and effective Bohr Radius $a^* = \frac{\hbar^2 \varepsilon}{m^* e^2}$ occurs when re-expressed in the unit system.

$$H = -\left(\frac{\partial^2}{\partial x^2} + \frac{\partial^2}{\partial y^2}\right) + \eta\, x + V(x,y) \tag{2}$$

Then , $\eta = |e|a^* F/R^*$ is defined as. By applying the finite difference method to the Schrödinger equation, energy levels E_n and wave functions Ψ_n are calculated by [5]:

$$H\psi_n(x,y) = E_n\psi_n(x,y) \tag{3}$$

In the finite different method, we have working on two dimensional axes. There are wave function for x- axes and y –axes and we have producted $\psi(x, y)$ from these wave functions. $\psi(x, y) = \psi(x).$ $\psi(y)$ it is defined as. In addition, there are energy states for both axes Ex and Ey. Total energy of the system E is sum of these energy states.
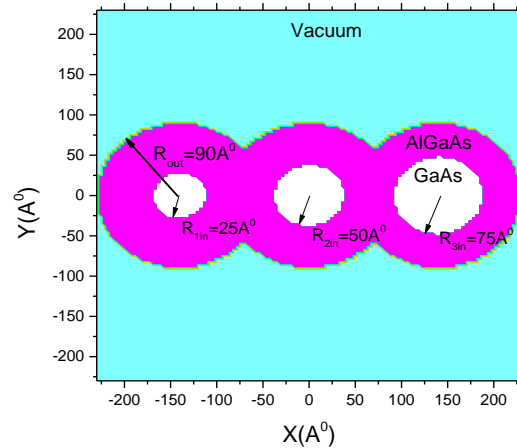

Figure 1. Planar cross-sectional view of quantum wire lattice.

By dividing both axes of the system by the number of n equal steps, we created a table of differences for wave functions
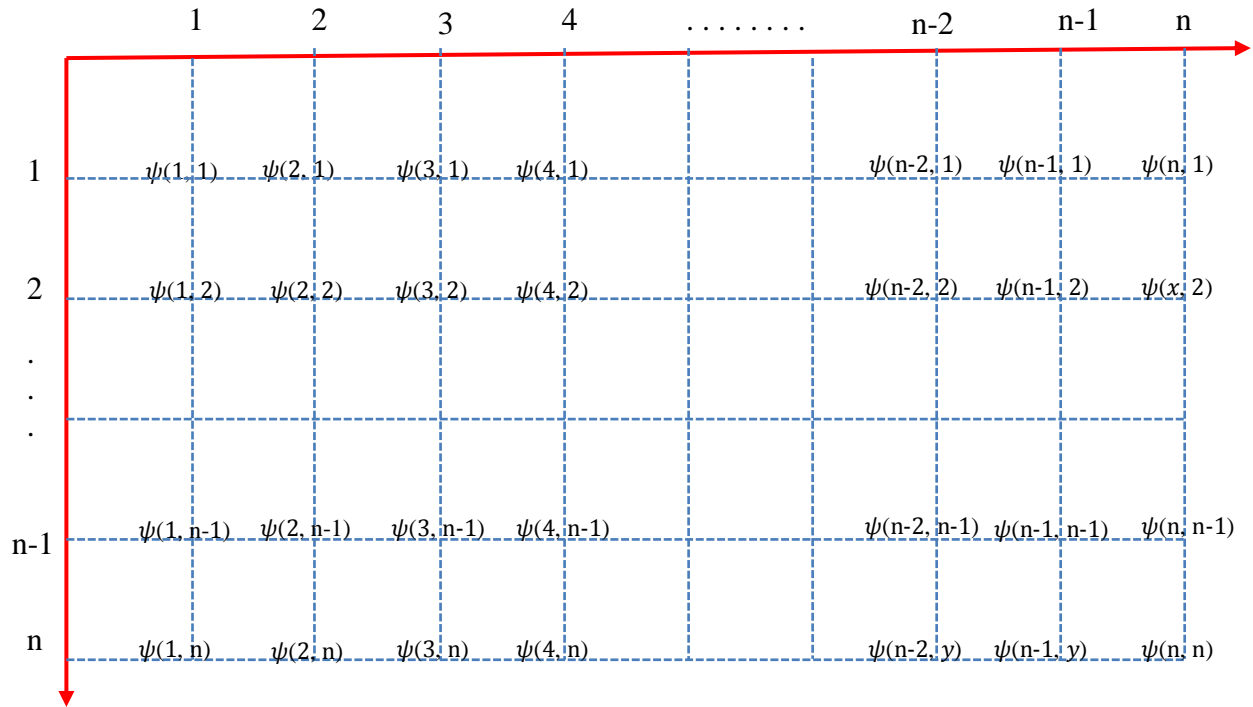
Figure 2. Table of differences for wave functions

The numerical derivative for the point ψ(1,1) becomes as.

$$\frac{1}{dx^2}\big(\psi(1,0) - 2\psi(1,1) + \psi(1,2)\big) - \frac{1}{dy^2}\big(\psi(0,1) - 2\psi(1,1) + \psi(2,1)\big) + V(1,1)\psi(1,1) =$$
$$\big(E_x + E_y\big)\psi(1,1) \tag{4}$$

If ψ(1,2), ψ(1,3)……ψ(n,n) is calculated again for the other points, we get a matrix of size n x n. This matrix is solved with a computer software. Wave functions and energy states are calculated from matrix

$$\begin{bmatrix} \frac{4}{dx^2} + V(1,1) & -\frac{1}{dx^2} & 0 & 0 & 0 & 0 & -\frac{1}{dy^2} & 0 & .. \\ -\frac{1}{dx^2} & \frac{4}{dx^2} + V(1,2) & -\frac{1}{dy^2} & 0 & 0 & 0 & 0 & -\frac{1}{dy^2} & 0 \\ 0 & -\frac{1}{dx^2} & \frac{4}{dx^2} + V(1,3) & -\frac{1}{dx^2} & 0 & 0 & 0 & . & . \\ & . & . & . & . & . & . & . & . \\ . & . & . & & . & . & . & . & . \\ ... & 0 & 0 & -\frac{1}{dy^2} & 0 & 0 & 0 & -\frac{1}{dx^2} & \frac{4}{dx^2} + V(n,n) \end{bmatrix} \begin{bmatrix} \psi(1,1) \\ \psi(1,2) \\ \psi(1,3) \\ . \\ : \\ . \\ \psi(n,n) \end{bmatrix} = E \begin{bmatrix} \psi(1,1) \\ \psi(1,2) \\ \psi(1,3) \\ . \\ : \\ . \\ \psi(n,n) \end{bmatrix}$$

Figure 3. 2D matrix form for finite different method

3. RESULT AND DISCUSSION

Potential profile calculations have numerically been calculated $m^* = 0,0665m_0$ for effective mass and dielectric constant $\varepsilon = 13,18$[21]. $Ga_{1-x}Al_xAs$ of barrier height for $x = 0,3$ Al concentration is $V_0 = 228meV$. The effective Bohr radius and Rydberg energy are $a^* = 104,88054$ A^o ve $R_y^* = 5,20848$ meV , respectively. Two different quantum wire lattices have been studied. In the first quantum wire lattice, the radius in the GaAs region are equal. Calculations were made for the sizes given in Figure 1 for the second quantum wire lattice.
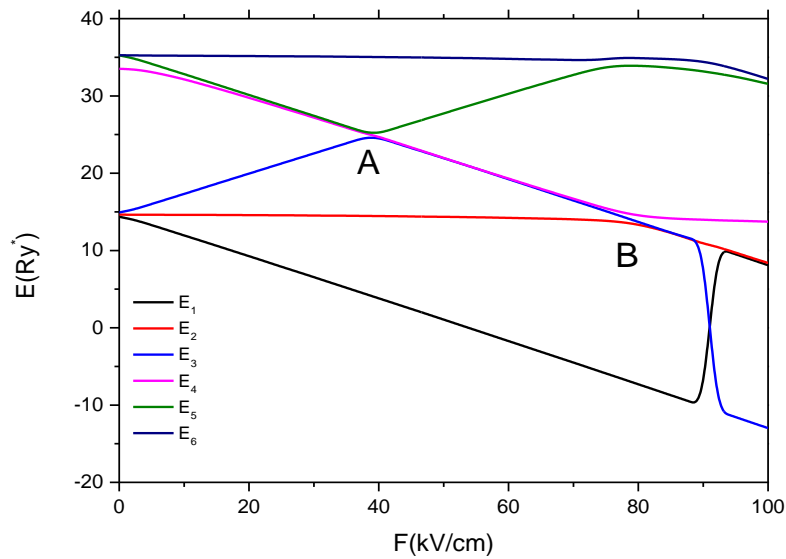
Figure 4. Energy levels of the GaAs region in a quantum wire lattice depending on the electric field for equal radius.
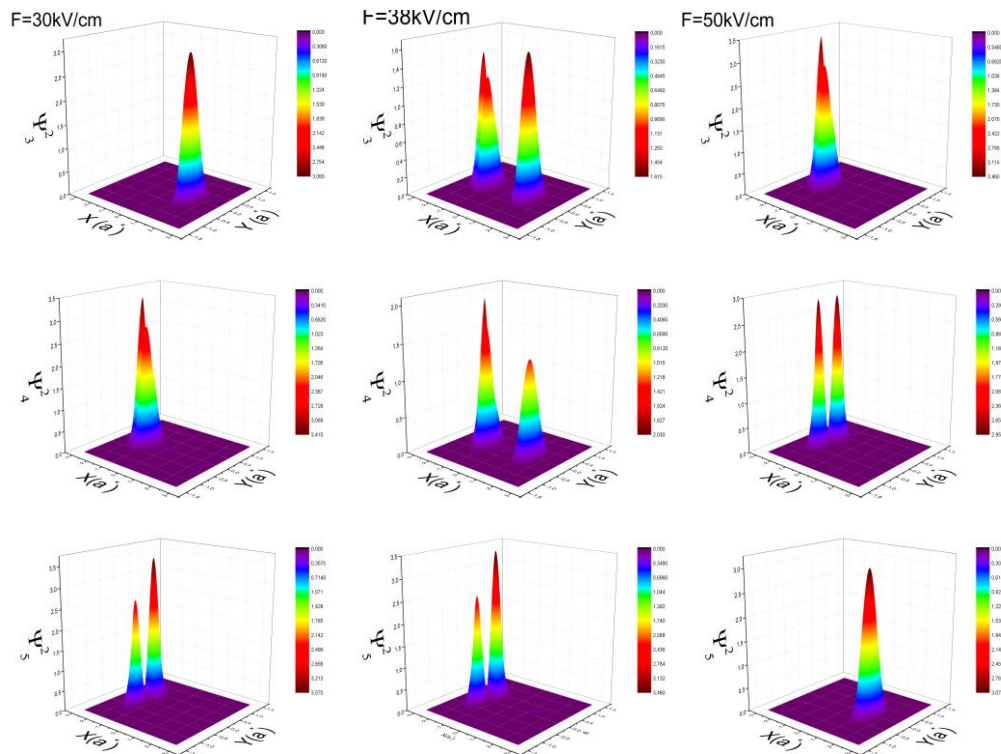

Figure 5. Probability of wave functions around point A

The variation of the energy levels with the electric field for equal radius and 50 A^o values of the GaAs region in the quantum wire lattice is shown by Figure 4. When the figure is investigated, it is seen that the first three energy levels are approximately at the same level for no electric field, and the levels exhibit different behaviors when electric field is applied. It has been observed that the energies approach each other at values where the electric field is 38 kV/cm (A point) and 78 kV/cm (B point). Electron probability distributions around these values are shown in Figure 5 and Figure 6 for point A and point B, respectively. If the energies tend to decrease with the electric field strength from these shapes, the electron will be in the left quantum wire of the probability distributions, while the energies tend to increase, the electron will be localized in the right quantum wire.
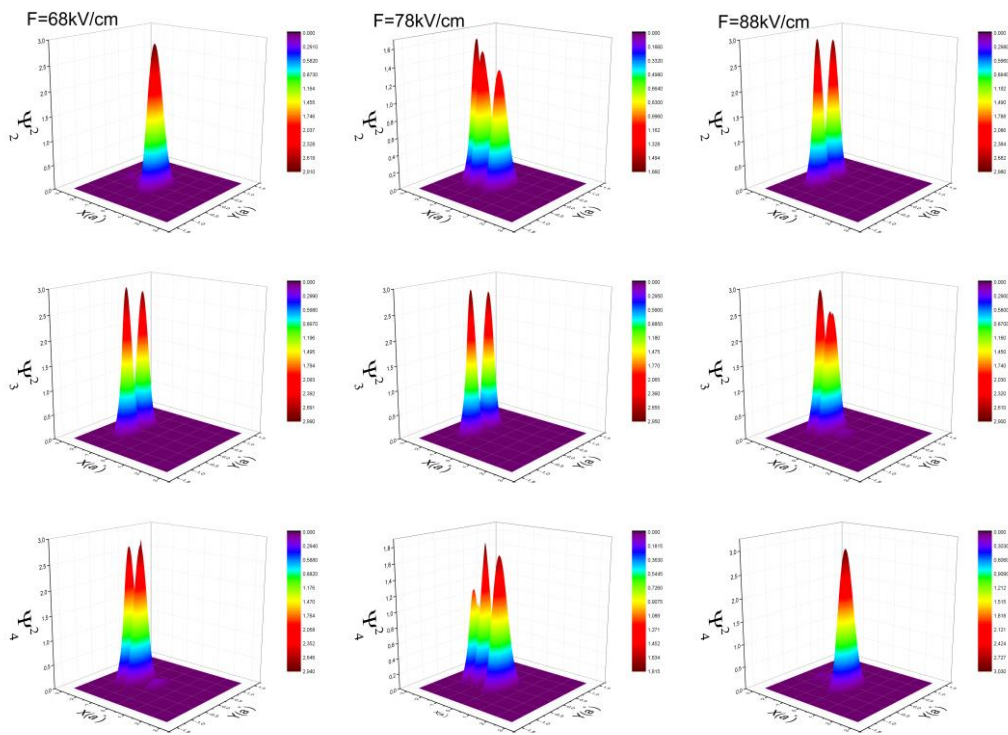

Figure 6. Probability of wave functions around point B

First six energy levels calculated from the ground state for the second quantum wire lattice, depending on the electric field strength showed by Figure 7. It has been observed that the energy levels converge to each other at certain values of the electric field. In the figure, the region A where the first two energy levels approach without crossing each other with an energy value of F=25 kV/cm, the same situation for the third, fourth and fifth energy levels, and the region B where the energy value for F=27 kV/cm, the second and fifth energy levels. For the third levels, the approach around F≅50 kV/cm is shown with the C state. As observed, when the behaviors of the energy levels under the electric field are compared with each other, the behaviors of the energy levels in Figure 4 do not exhibit similar characteristics.
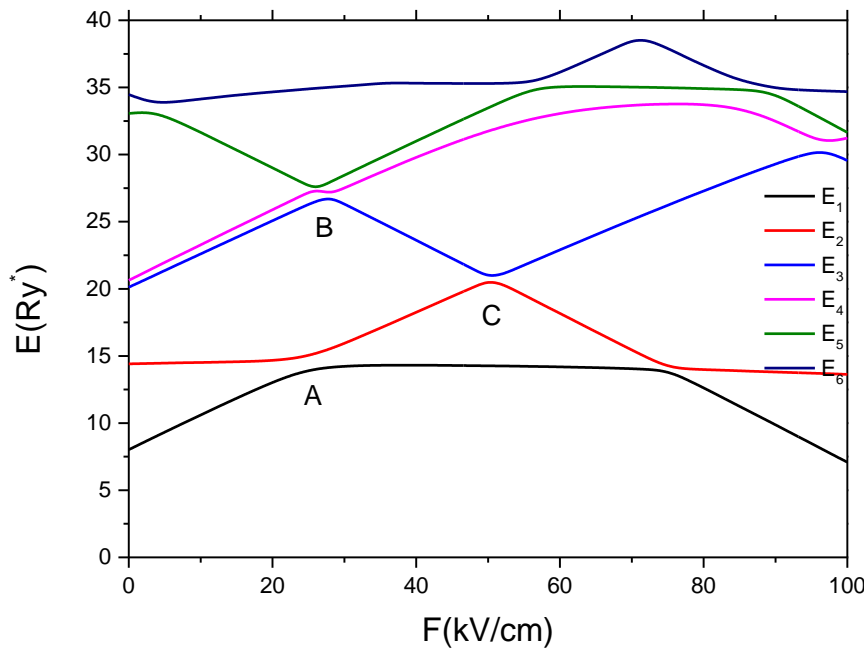

Figure 7. Variation of energy levels of the GaAs region in the quantum wire lattice depending on the electric field for different radius.

In Figure 8, the probability distributions in the first two energy levels for F=15 kV/cm before the energy approach, F=25 kV/cm at the approach point and F=40kV/cm after the energy approach at point A marked in Figure 7 are shown as the C state. While the ψ_1^2 ground state probability densities are localized to the right wire, which is the largest area of the GaAs region, for electron 15 kV/cm,

it is observed that it is localized towards the middle wire with the increase in electric field strength. In the second energy, it has been observed that the electron probability density is localized from the inner wire to the right outer wire, with the increase of a certain electric field strength, both between these levels and when these levels are compared with the first levels, without disturbing the orthogonality condition. When these probability densities are considered, it has been observed that the electron probability densities are in the same regions at both energy levels at F=25kV/cm. At the value of F=35kV/cm, it is seen that the wavefunction densities of both energy states are in the opposite state of the densities of the F=15kV/cm wavefunctions.
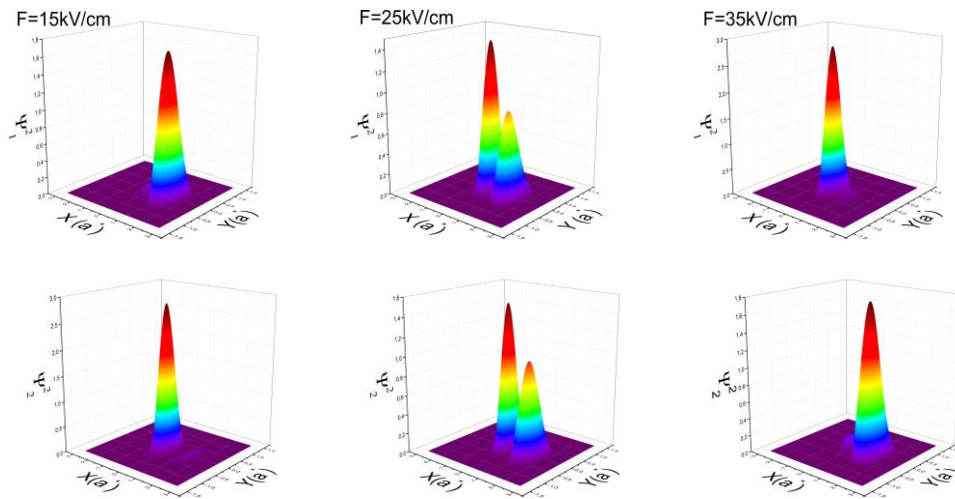
Figure 8. Probability of wave functions around point A

In Figure 9, electron probability densities of the third, fourth and fifth energy levels are given for the electric field values in and around the point B in Figure 7. When the ψ_3^2 and ψ_4^2 electron probability densities at F= 15 kV/cm are investigated, they are localized in the same wire, while ψ_5^2 electron probability densities are localized on the left wire. In this electric field strength value, E3 and E4 energies increase while E5 energy decreases. At the value of F= 27kV/cm, the E3 and E5 energies are close to each other and the electron probability densities are higher in the right wire. Since it shows a decrease according to the E4 energy value, the probability density is on the left string. At F= 39kV/cm, E4 and E5 energies increased and probability densities were located

on the right wire. The E3 energy is decreased and the electron probability density is located in the left wire.
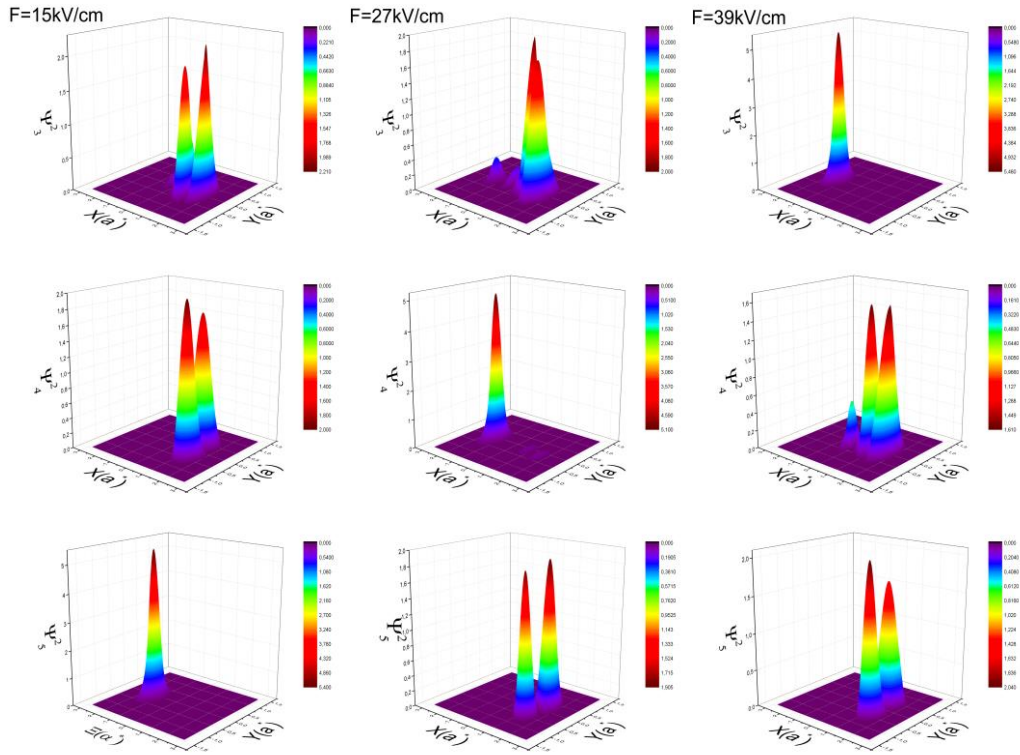

Figure 9. Probability of wave functions around point B

In Figure 10, the probability densities of the second and third energy levels are given for the electric field values at and around point C in Figure 5. At F= 40kV/cm, E2 energy tends to increase, E3 energy tends to decrease, and when ψ_2^2 and ψ_3^2 electron probability densities are examined, it is seen that they are localized in different wires. When the electric field is increased, the behavior of the energies is reversed, and the electron probability density of ψ_2^2 at F=60 kV/cm is localized on the left-hand wire, while the ψ_3^2 electron probability density is localized on the right-hand wire.
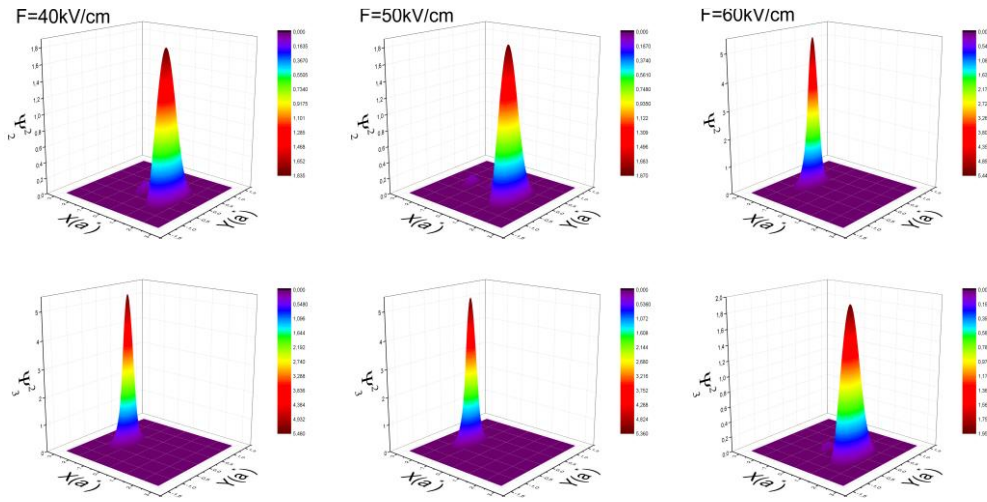
Figure 10. Probability of finding wave functions around point C.

4. CONCLUSION

In this study, three $Ga_{1-x}Al_xAs/GaAs$ cylindrical quantum wires are brought together to form a $Ga_{1-x}Al_xAs/GaAs$ quantum wire lattice. In this structure, two different quantum wire lattices have been studied by taking the radius of the GaAs material as equal and different. Both wire lattices showed interesting changes in their energy states with the change of the electric field. To explain the interestingness in these energy changes, probability distributions of states at certain electric field values are plotted. When we look at other studies in the literature, it is seen that the geometry of the structure is as important as the external field applied to semiconductor materials [17,18,21]. Energy transitions are only possible with the correct geometry selection. These approach points in energy levels can be considered as transition points and these points can be designed as switching elements in electronic devices. The results are expected to be guiding in designing new structures in terms of diversifying the electronic properties of semiconductor low-dimensional structures.

Note: This article has presented as oral presentation at NEM 2022 Kırklareli

REFERENCES

[1] Montes, A., Duque, C. A., & PorrasMontenegro, N. (1997). The binding energies of shallow donor impurities in GaAs quantum-well wires under applied electric fields. Journal of Applied Physics, 81(12), 7890-7894.

[2] Duque, C. A., Montes, A., & Morales, A. L. (2001). Binding energy and polarizability in GaAs-(Ga,Al)As quantum-well wires. Physica B, 302, 84-87.

[3] Aktas S., Okan S. E., & Akbas, H. (2001). Electric field effect on the binding energy of a hydrogenic impurity in coaxial GaAs/AlxGa1-xAs quantum well-wires. Superlattices and Microstructures, 30(3), 129-134.

[4] Aktas, Ş., Boz F.K., Bilekkaya A., S.E. Okan, The electronic properties of a coaxial square GaAs/AlxGa1−xAs quantum well wire in an electric field, Physica E: Low-dimensional Systems and Nanostructures, Volume 41, Issue 8, 2009, Pages 1572-1576

[5] Bilekkaya, A., Aktas, S., Okan, S. E., & Boz, F. K. (2008). Electric and magnetic field effects on the binding energy of a hydrogenic impurity in quantum well wires with different shapes. Superlattices and Microstructures, 44(1), 96-105.

[6] Mughnetsyan, V. N., Barseghyan, M. G., & Kirakosyan, A. A. (2008). Binding energy and photoionization cross section of hydrogen-like donor impurity in quantum well-wire in electric and magnetic fields. Superlattices and Microstructures, 44(1), 86-95.

[7] Kasapoglu, E., Yesilgul, U., Sari, H., & Sokmen, I. (2005). The effect of hydrostatic pressure on the photoionization cross-section and binding energy of impurities in quantum-well wire under the electric field. Physica B-Condensed Matter, 368(1-4), 76-81.

[8] Baser, P., Elagoz, S., & Baraz, N. (2011). Hydrogenic impurity states in zinc-blende InxGa1-xN/GaN in cylindrical quantum well wires under hydrostatic pressure. Physica E-Low-Dimensional Systems & Nanostructures, 44(2), 356-360.

[9] Çiçek E., Mese A. I., Ozkapi B., & Erdoğan I.(2021). Combined effects of the hydrostatic pressure and temperature on the self-polarization in a finite quantum well under laser field. Superlattices and Microstructures, Volume 155, July 2021, 106904

[10] Khordad, R. (2009). Effect of temperature on the binding energy of excited states in a ridge quantum wire. Physica E-Low-Dimensional Systems & Nanostructures, 41(4), 543-547.

[11] Kasapoglu, E., Ungan, F., Sari, H., & Sokmen, I. (2010). The hydrostatic pressure and temperature effects on donor impurities in cylindrical quantum wire under the magnetic field. Physica E-Low-Dimensional Systems & Nanostructures, 42(5), 1623-1626.

[12] Niculescu, E. C., Burileanu, L. M., & Radu, A. (2008). Density of impurity states of shallow donors in a quantum well under intense laser field. Superlattices and Microstructures, 44(2), 173-182.

[13] Niculescu, E. C., Burileanu, L. M., Radu, A., & Lupascu, A. (2011). Anisotropic optical absorption in quantum well wires induced by high-frequency laser fields. Journal of Luminescence, 131(6), 1113-1120.

[14] Boz F. K., Aktas S., Bekar B., & Okan, S. E. (2012). Laser field-driven potential profiles of double quantum wells. Physics Letters A, 376(4), 590-594.

[15] Kasapoglu, E., Sari, H., Yesilgul, U., & Sokmen, I. (2006). The effect of intense laser field on the photoionization cross-section and binding energy of shallow donor impurities in graded quantum-well wire under an electric field. Journal of Physics-Condensed Matter, 18(27), 6263-6271.

[16] Narayani, V., & Sukumar, B. (1994). Polarizability of a Shallow Donor in a Quantum-Well Wire- Geometric Effects. Solid State Communications, 90(9), 575-579.

[17] Ulas, M., Akbas, H., & Tomak, M. (1997). Shallow donors in a quantum well wire: Electric field and geometrical effects. Physica Status Solidi B-Basic Solid State Physics, 200(1), 67-73.

[18] Ulas, M., Erdogan, I., Cicek, E., & Dalgic, S. S. (2005). Self polarization in GaAs-(Ga, Al)As quantum well wires: electric field and geometrical effects. Physica E-Low-Dimensional Systems & Nanostructures, 25(4), 515-520.

[19] Akankan, O., Erdogan, I., Mese, A.I. et al. (2021) The effects of geometrical shape and impurity position on the self-polarization of a donor impurity in an infinite GaAs/AlAs tetragonal quantum dot. Indian Journal of Physics 95, 1341–1344.

[20] Mese A, I., Cicek E., Erdogan I., Akankan O., and H Akbas, (2017). The effect of dielectric constant on binding energy and impurity self-polarization in a GaAs–$Ga_{1-x}Al_xAs$ spherical quantum dot, Indian Journal of Physics 91(3):263–268

[21] Bekar B., Boz F.K., Aktas B., & Okan S. E. (2019). The Effect on the Optical Absorption Coefficients due to the Positions in the Plane of Square GaAs /Al(GaAs) Quantum Well Wire under the Laser Field. Acta Physıca Polonıca A 136(6), 882-88.